



HAL
open science

Hydrous magmatism triggered by assimilation of hydrothermally altered rocks in fossil oceanic crust (northern Oman ophiolite)

Lyderic France, Benoit Ildefonse, Juergen Koepke

► To cite this version:

Lyderic France, Benoit Ildefonse, Juergen Koepke. Hydrous magmatism triggered by assimilation of hydrothermally altered rocks in fossil oceanic crust (northern Oman ophiolite). *Geochemistry, Geophysics, Geosystems*, 2013, 14 (8), pp.2598-2614. 10.1002/ggge.20137 . hal-00939400

HAL Id: hal-00939400

<https://hal.science/hal-00939400>

Submitted on 20 Dec 2021

HAL is a multi-disciplinary open access archive for the deposit and dissemination of scientific research documents, whether they are published or not. The documents may come from teaching and research institutions in France or abroad, or from public or private research centers.

L'archive ouverte pluridisciplinaire **HAL**, est destinée au dépôt et à la diffusion de documents scientifiques de niveau recherche, publiés ou non, émanant des établissements d'enseignement et de recherche français ou étrangers, des laboratoires publics ou privés.

Copyright



Hydrous magmatism triggered by assimilation of hydrothermally altered rocks in fossil oceanic crust (northern Oman ophiolite)

Lydéric France

CRPG, UMR 7358, CNRS, Université de Lorraine, Vandoeuvre-lès-Nancy France (lyde@crpg.cnrs-nancy.fr)

Benoit Ildefonse

Géosciences Montpellier, CNRS, Université Montpellier 2, Montpellier, France

Juergen Koepke

Institut fuer Mineralogie, Universitaet Hannover, Hannover, Germany

[1] Mid-ocean ridges magmatism is, by and large, considered to be mostly dry. Nevertheless, numerous works in the last decade have shown that a hydrous component is likely to be involved in ocean ridges magmas genesis and/or evolution. The petrology and geochemistry of peculiar coarse grained gabbros sampled in the upper part of the gabbroic sequence from the northern Oman ophiolite (Wadi Rajmi) provide information on the origin and fate of hydrous melts in fast-spreading oceanic settings. Uncommon crystallization sequences for oceanic settings (clinopyroxene crystallizing before plagioclase), extreme mineral compositions (plagioclase An% up to 99, and clinopyroxene Mg # up to 96), and the presence of magmatic amphibole, imply the presence of a high water activity during crystallization. Various petrological and geochemical constraints point to hydration, resulting from the recycling of hydrothermal fluids. This recycling event may have occurred at the top of the axial magma chamber where assimilation of anatectic hydrous melts is recurrent along mid-ocean ridges or close to segments ends where fresh magma intrudes previously hydrothermally altered crust. In ophiolitic settings, hydration and remelting of hydrothermally altered rocks producing hydrous melts may also occur during the obduction process. Although dry magmatism dominates oceanic magmatism, the dynamic behavior of fast-spreading ocean ridge magma chambers has the potential to produce the observed hydrous melts (either in ophiolites or at spreading centers), which are thus part of the general mid-ocean ridges lineage.

Components: 9,429 words, 9 figures, 1 table.

Keywords: fast-spreading mid-ocean ridges; Oman ophiolite; melt lens; contamination; axial magma chamber; gabbro.

Index Terms: 3614 Mineralogy and Petrology: Mid-oceanic ridge processes; 3625 Mineralogy and Petrology: Petrography, microstructures, and textures; 3640 Mineralogy and Petrology: Igneous petrology.

Received 7 November 2012; **Revised** 29 March 2013; **Accepted** 3 April 2013; **Published** 1 August 2013.

France, L., B. Ildefonse, and J. Koepke (2013), Hydrous magmatism triggered by assimilation of hydrothermally altered rocks in fossil oceanic crust (northern Oman ophiolite), *Geochem. Geophys. Geosyst.*, 14, 2598–2614, doi:10.1002/ggge.20137.

1. Introduction

1.1. Magmatic Accretion at Fast-Spreading Ridges

[2] Oceanic crust represents about two thirds of the Earth surface, and nearly half of it formed at fast-spreading ridges. The structure and composition of oceanic crust are constrained by off-shore geophysical studies, in situ geological mapping and sampling (dredging, drilling, submersible, and ROV studies), and studies of ophiolitic complexes. Geophysical studies of fast-spreading ridges, primarily the East Pacific Rise [e.g., Morton and Sleep, 1985; Detrick et al., 1987], have shown that the ridge axis is composed of a magma chamber at depth (containing less than 20% of melt according to Lamoureaux et al. [1999]), which is overlaid by a thin and narrow, mostly liquid, melt lens at its top (Figure 1). Above, the upper crust forms an upper lid with the sheeted dyke complex and volcanics. The upper crust is considered to be mostly fed by the upper melt lens [MacLeod and Yaouancq, 2000; Koepke et al., 2011; Wanless and Shaw, 2012], while the lower crust is probably fed from the top (melts from the upper melt lens; Phipps Morgan and Chen [1993], Quick and Denlinger [1993], Coogan [2003], and Nicolas et al. [2009]), or from the bottom (melts from the mantle; Kelemen et al. [1997]), or from top and bottom [Boudier et al., 1996]. Understanding active processes in and around the axial melt lens is therefore of major importance to constrain magmatic dynamics of fast-spreading ridge systems. This melt lens is a dynamic horizon that can migrate upward and downward, with the potential to reheat, dehydrate, and sometimes to melt and/or assimilate the previously hydrothermally altered sheeted dike complex base [Phipps Morgan and Chen, 1993; Hoofst et al., 1997; Gillis and Coogan, 2002; Coogan et al., 2003, Gillis, 2008; Koepke et al., 2008; France et al., 2009, 2010]. When moving down after the termination of a magmatic pulse or when moving off-axis, the melt lens crystallizes to form typical “isotropic gabbros” horizon (Figure 1) [Pallister and Hopson, 1981; Sinton and Detrick, 1992; Natland and Dick, 1996; MacLeod and Yaouancq, 2000; France et al., 2009; Koepke et al., 2011]. The study of this horizon at the interface between the lower and the upper crust therefore provides the opportunity to study in situ the processes occurring within and around the melt lens. This horizon is only accessible in ophiolites [MacLeod and Yaouancq, 2000; Nicolas et al., 2008; France

et al., 2009], in the recent crust by in situ drilling [e.g., Wilson et al., 2006], at tectonic windows that expose the gabbroic crust [e.g., Natland and Dick, 1996], and through analyses of mineral-hosted melt inclusions from ocean floor basalts [e.g., Wanless and Shaw, 2012].

[3] Oceanic spreading centers are historically considered to represent “dry and reducing magmatic systems” opposed to the “wet and oxidizing” suprasubduction environments [e.g., Sobolev and Chaussidon, 1996; Wood et al., 1990; Kelley and Cottrell, 2009]. Nevertheless several studies conducted on present day oceanic crust [Michael and Schilling, 1989; Michael and Cornell, 1998; Nielsen et al., 2000; Koepke et al., 2004, 2005a, 2005b, 2007, 2011; Berndt et al., 2005; Cordier et al., 2007; France et al., 2009, 2010] and on ophiolites [Benoit et al., 1999; Koga et al., 2001; Gillis and Coogan, 2002; Nicolas et al., 2008; France et al., 2009; Koepke et al., 2009; Abily et al., 2011] have shown that a hydrous component may be involved in the genesis of mid-ocean ridge basalts (MORBs). Hydration may be associated with seawater-magma interactions during seafloor emplacement, with hydrothermally altered crust-magma interactions at magma chamber margins, with ridge tectonics, and/or with obduction processes in the case of ophiolites [e.g., Michael and Schilling, 1989; Boudier et al., 2000; Bosch et al., 2004; France et al., 2009; Koepke et al., 2009; Abily et al., 2011].

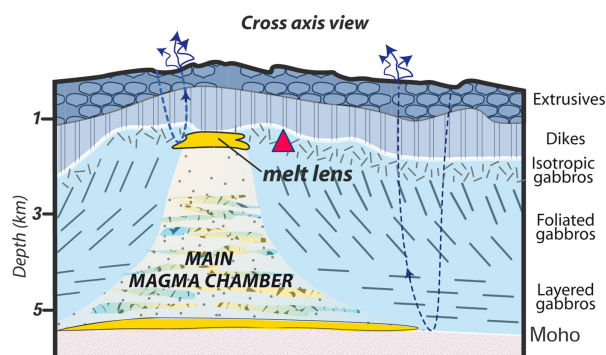


Figure 1. Schematic cross-axis view of the magmatic system present at fast-spreading ridges (modified after France et al. [2009]). From top to bottom, crust is composed of extrusives and dikes (forming the upper crust), and isotropic, vertically foliated, and horizontally layered gabbros (forming the lower crust). The main magma chamber is composed of a mush containing less than 20% of melt, topped by an upper melt lens that is mostly filled with near pure liquid. Dashed blue curves identify hydrothermal circulation. Red triangle shows the level from where the investigated gabbros in the Wadi Rajmi originated.

[4] The present study focuses on the origin of some coarse-grained gabbros sampled in the isotropic gabbro horizon in the Wadi Rajmi of the northern Oman ophiolite. These samples have been selected for their peculiar petrology following intense investigations of isotropic gabbro horizon in the Oman ophiolite [France, 2009; Nicolas et al., 2008; France et al., 2009; Nicolas et al., 2009]. Across the whole ophiolite, this horizon (also called *varitextured gabbro horizon*) is heterogeneous and represents different generations of melts crystallizing in close association [e.g., MacLeod and Yaouancq, 2000; Koepke et al., 2011]. The horizon of isotropic gabbros is composed of fine-grained isotropic gabbros, which is the main lithology, some subordinated coarse-grained gabbros, some screens of vertically foliated gabbro (with respect to the assumed paleo-ocean floor [see Figures 6 in MacLeod and Yaouancq, 2000]), Fe-Ti-gabbros, and leucocratic rocks [MacLeod and Yaouancq, 2000; France et al., 2009]. The origin of the coarse-grained gabbro is attributed to either in situ fractionation of basaltic liquids under reducing conditions (relative to classical mid-ocean ridges melts), enabling the formation of melts enriched in FeO and TiO₂ [MacLeod and Yaouancq, 2000], or to the crystallization of melts generated by hydrous partial melting of still hot lithologies during an influx of hydrothermal fluid at magmatic temperatures [Nicolas et al., 2008]. Samples studied by both author groups are not similar from a mineralogical point of view. MacLeod and Yaouancq [2000] have described Fe-Ti-gabbros that cannot be generated by hydrous partial melting of mafic lithologies, as such anatectic melts are Ti-depleted [Koepke et al., 2004]. On the contrary, Nicolas et al. [2008] described coarse-grained gabbros crystallized from a hydrous and oxidizing magma that cannot be generated under dry and reducing conditions. Both hypotheses are thus probably correct and not mutually exclusive. MacLeod and Yaouancq [2000], and Nicolas et al. [2008] described these coarse-grained gabbros as irregular blebs, pockets, patches, or veins (up to 50 cm) occurring in finer-grained gabbros. The present study aims to decipher on the origin of newly sampled coarse-grained gabbros and to replace their genesis in the general frame of oceanic crust formation.

1.2. Regional Settings

[5] The Cretaceous Oman ophiolite is regarded as the best example for fast-spreading oceanic crust on land. Nevertheless, a controversial debate is

ongoing since decades, opposing the mid-ocean ridge to a suprasubduction zone initial setting [e.g., Stern, 2004; Warren et al., 2005; Boudier and Nicolas, 2007; Warren et al., 2007]. If a subduction zone-related environment is accepted for a part of the Oman ophiolite, the nature of this subduction zone is still under discussion. Most authors propose that the subduction process is linked to the early stage of obduction [e.g., Boudier et al., 1988; Koepke et al., 2009], and is responsible for a second stage of magmatism (“V2” or “Lasail” lavas; Alabaster et al. [1982], Ernewein et al. [1988], and Yamasaki et al. [2006]) following the main major accretion of normal fast-spread crust (“V1” or “Geotimes” lavas; Alabaster et al. [1982] and Ernewein et al. [1988]). The main difference between lavas is that the V2 lavas are interpreted as resulting from fluid-enhanced melting of previously depleted mantle and contrast in composition with the V1 lavas that resemble modern MORB (for details and nomenclature of the lavas see Godard et al. [2003]). The coarse-grained gabbros studied herein were sampled in the Wadi Rajmi area in the northern Fizh massif of the Oman ophiolite (Figure 2). It is located close to a segment tip, and large, subvertical shear zones are observed in the mantle [Nicolas et al., 2000, Nicolas and Boudier, 2008] and crustal sections [Reuber, 1988].

[6] In the Wadi Rajmi area, oceanic crust is roughly 8 km thick [Usui and Yamazaki, 2010]. From west to east, are exposed, harzburgites from the mantle section, and layered, foliated, and isotropic gabbros, overlain by a sheeted dike complex, and lavas forming the crustal sequence. These lithologies are considered to represent the normal crustal sequence (V1-MORB like magmas; Alabaster et al. [1982] and Ernewein et al. [1988]). A second magmatic stage (with V2-suprasubduction like magmas) has been identified in the area; it is represented from west to east by intrusions of massive and layered ultramafic rocks, gabbronorites, and plagiogranites, and by the upper lava sequence typical of island arc with some boninites flows [Ishikawa et al., 2002]. Suprasubduction like plutonics and volcanics are connected by an andesitic and boninitic dike network [Yamazaki and Miyashita, 2008]. The second magmatic stage seems to be related to a second-order segmentation feature (e.g., similar to overlapping spreading centers at the East Pacific Rise) of the spreading ridge [Boudier et al., 2000; MacLeod and Rothery, 1992]. Alternatively, this second magmatic phase can be related to the

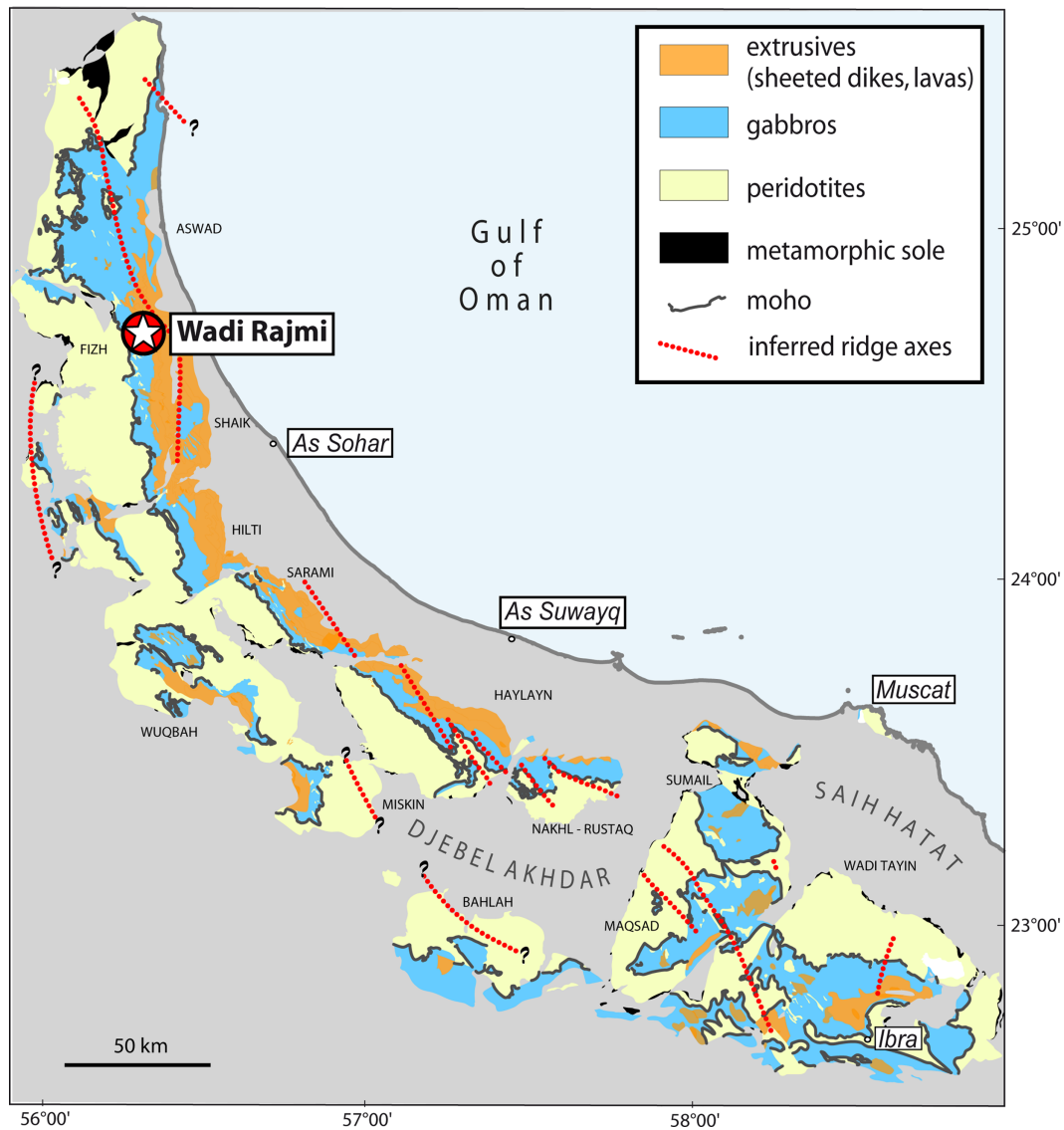


Figure 2. Simplified geological map of the Oman ophiolite and location of the Wadi Rajmi area in the Fizh massif (modified after *Nicolas et al.* [2000]).

beginning of obduction [*Ishikawa et al.*, 2002; *Yamasaki et al.*, 2006; *Koepke et al.*, 2009].

2. Samples and Results

[7] In Wadi Rajmi, the isotropic gabbro horizon is highly complex with some olivine gabbros, gabbros, gabbroonorites, and locally some plagiogranites. The rocks typically vary in grain sizes from hundreds of micrometers to several centimeters; most are fine to coarse grained. Here we focus on two coarse-grained gabbros (07OL34 and 07OL36) with peculiar characteristics, which have been sampled in this horizon in Wadi Rajmi, thus corresponding to frozen parts of the axial melt lens

(coordinates: 431 157E; 2 724 497N; 261 m, and 430 565E; 2 723 695N; 285 m, respectively). Gabbro 07OL34 was sampled in a coarse-grained gabbro patch (~1.5 m wide) intruding a fine-grained isotropic gabbro. Gabbro 07OL36 is a spotty coarse-grained gabbroonorite containing orthopyroxene megacrysts; it intrudes a fine-grained isotropic gabbro that is characteristic of the isotropic gabbro horizon (Figure 3). In this outcrop, thin leucocratic dikelets are observed intruding fine-grained isotropic gabbro.

2.1. Petrography

[8] Sample 07OL34 displays a general granular texture with large prismatic clinopyroxene and

plagioclase grains (5 and 3 mm on average, respectively; Figures 4a–4d). Plagioclase grains contain numerous small (150 μm on average) isolated clinopyroxene inclusions (Figures 4a–4d). Backscattered electron (BSE) images show that clinopyroxene grains are zoned. The inclusions display a zonation with a relatively sharp contact between the core and the rim (Figures 5a and 5b). The large, prismatic clinopyroxene grains display heterogeneous inner parts of the crystals and a thin (<100 μm) homogeneous rim (Figures 5c–5d).

[9] The spotty coarse-grained gabbronorite 07OL36 displays two lithological domains organized as patches (5–10 mm wide), which are homogeneously distributed in the sample (Figure 6). One domain (hereafter “P domain,” with “P” standing for poikilitic) is composed of large poikilitic plagioclase grains (5 mm in average, up to 10 mm), which contain smaller granular clinopyroxene chadacrysts (0.4 mm in average; Figures 4e, 4f, 5e, 5f, and 6). Some poikilitic orthopyroxene and amphibole grains (7 and 5 mm, respectively) containing similar granular clinopyroxene chadacrysts are also observed associated to P domains (Figure 6). The other domain (hereafter “G domain,” with “G” standing for granular) is mainly composed of granular clinopyroxene grains (0.6 mm in average) containing tiny oxide inclusions (0.1–10 μm) and subordinated amphibole blebs (Figures 5f and 6). Close to the contact between the two domains, some clinopyroxene grains containing tiny oxide inclusions (typical of G domain) are included in the poikilitic plagioclases (typical of P domain). Some quartz is locally observed.

2.2. Phase Composition

[10] Major element mineral analyses (Table 1) were performed using a Cameca SX100 electron microprobe (Géosciences Montpellier) equipped with five spectrometers and an operating system “Peak sight.” All data were obtained using a 15 kV acceleration potential, a static (fixed) beam, $K\alpha$ emission from all elements, and a matrix correction based on *Pouchou and Pichoir* [1991] and [Merlet, 1994]. The crystals were analyzed with a beam current of 10 nA using a focused beam and a counting time of 15 s on background and 30 s on peak. BSE images (Figure 5) were obtained on the same CAMECA SX100 electron microprobe. WDX X-ray mappings (Figure 6) were obtained using the imaging program of the CAMECA software package “Peaksight” and combined using Adobe Photoshop® and Adobe Illustrator® soft-

wares. Data presented below are averages associated to their standard deviation.

[11] In 07OL34, plagioclases have An contents up to 99% ($\text{An}\% = 96 \pm 6$; with $\text{An}\% = \text{Ca}/(\text{Ca} + \text{Na} + \text{K})$ in molar proportions); no core-rim variation has been observed. As noted earlier, this sample shows two types of clinopyroxenes: chadacrysts within the large plagioclase and large prismatic crystals (Figures 5a–5d), which show significant differences in their composition. The cores of the chadacrysts present in the large plagioclase grains (Figure 5a–5b; bright colors in the BSE images) are relatively enriched in FeO ($\text{Mg}\# = 83$; with $\text{Mg}\# = \text{Mg}/(\text{Mg} + \text{Fe})$ in molar proportions), while the rims (Figures 5a–5b; dark on the BSE images) are strongly enriched in MgO ($\text{Mg}\# = 92 \pm 2$). The rims of the large, prismatic clinopyroxene (Figures 5c–5d) are also enriched in MgO ($\text{Mg}\# = 92 \pm 1$), while the central parts of these are quite heterogeneous, with compositions ranging in Mg # between 83 and 92. Amphiboles vary continuously from actinolites to hornblendes.

[12] In 07OL36, minerals from P and G domains display different compositions. Granular clinopyroxenes included in the poikilitic plagioclases of P domains have similar Mg #, and higher Al_2O_3 (1.93 ± 0.19 wt %), TiO_2 (0.39 ± 0.10 wt %), and Cr_2O_3 (0.24 ± 0.05 wt %), and lower CaO (22.02 ± 0.38 wt %) contents than the oxide-bearing clinopyroxenes from G domains (0.86 ± 0.31 , 0.19 ± 0.09 , 0.10 ± 0.05 , and 23.13 ± 0.82 wt %, respectively). At G domains margin, close to P domains, oxide-bearing clinopyroxenes have rims with compositions similar to P domains clinopyroxenes. In both domains, clinopyroxenes have $\text{Mg}\# = 77.5 \pm 1$, plagioclases have An contents up to



Figure 3. Outcrop showing the sampling area of sample 07OL36 (star). Two main facies are observed: a fine-grained gabbro (central part of the picture) and a spotty coarse-grained one containing orthopyroxene megacrysts.

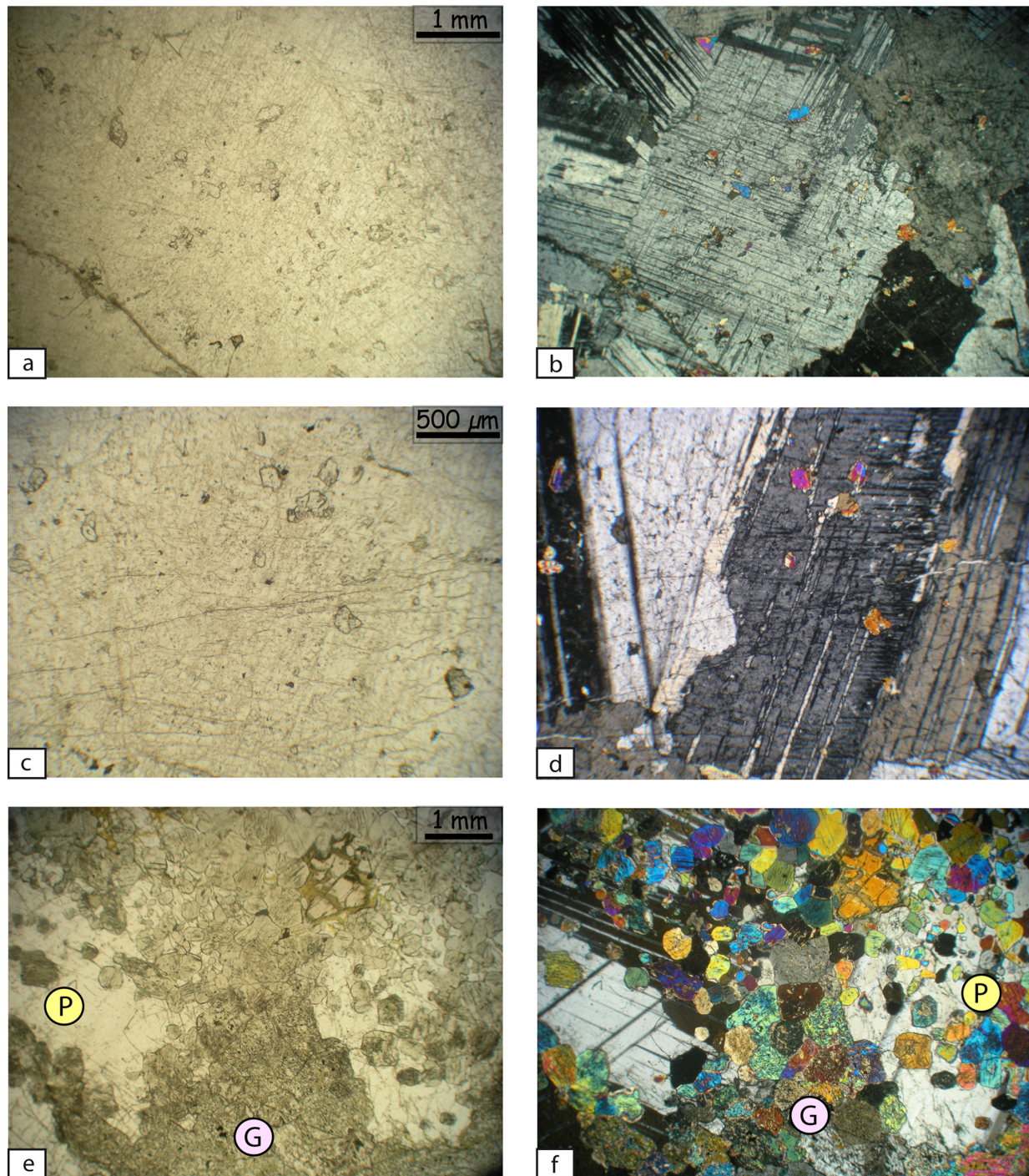


Figure 4. Microphotographs of samples (a–d) 07OL34 and (e and f) 07OL36; plane-polarized light for Figures 4a, 4c, and 4e, and cross-polarized light for Figures 4b, 4d, and 4f). Figures 4a–4d: large plagioclase grains containing numerous isolated clinopyroxene inclusions. Figures 4e and 4f: 07OL36 gabbro-norite contains two domains, P domain contains poikilitic plagioclase grains that include several individual granular clinopyroxene chadacrysts that are devoid of oxide and G domains exclusively composed of clinopyroxenes containing tiny oxide inclusions and subordinated amphiboles.

93 (88 ± 3), orthopyroxene are enstatite with $Mg \# = 70 \pm 2$, and amphibole vary continuously from actinolites, through hornblende to edenite, with an average value of $Mg \# = 79 \pm 4$.

3. Thermometry

[13] Various geothermometers have been used to estimate the equilibrium temperatures. In 07OL34,

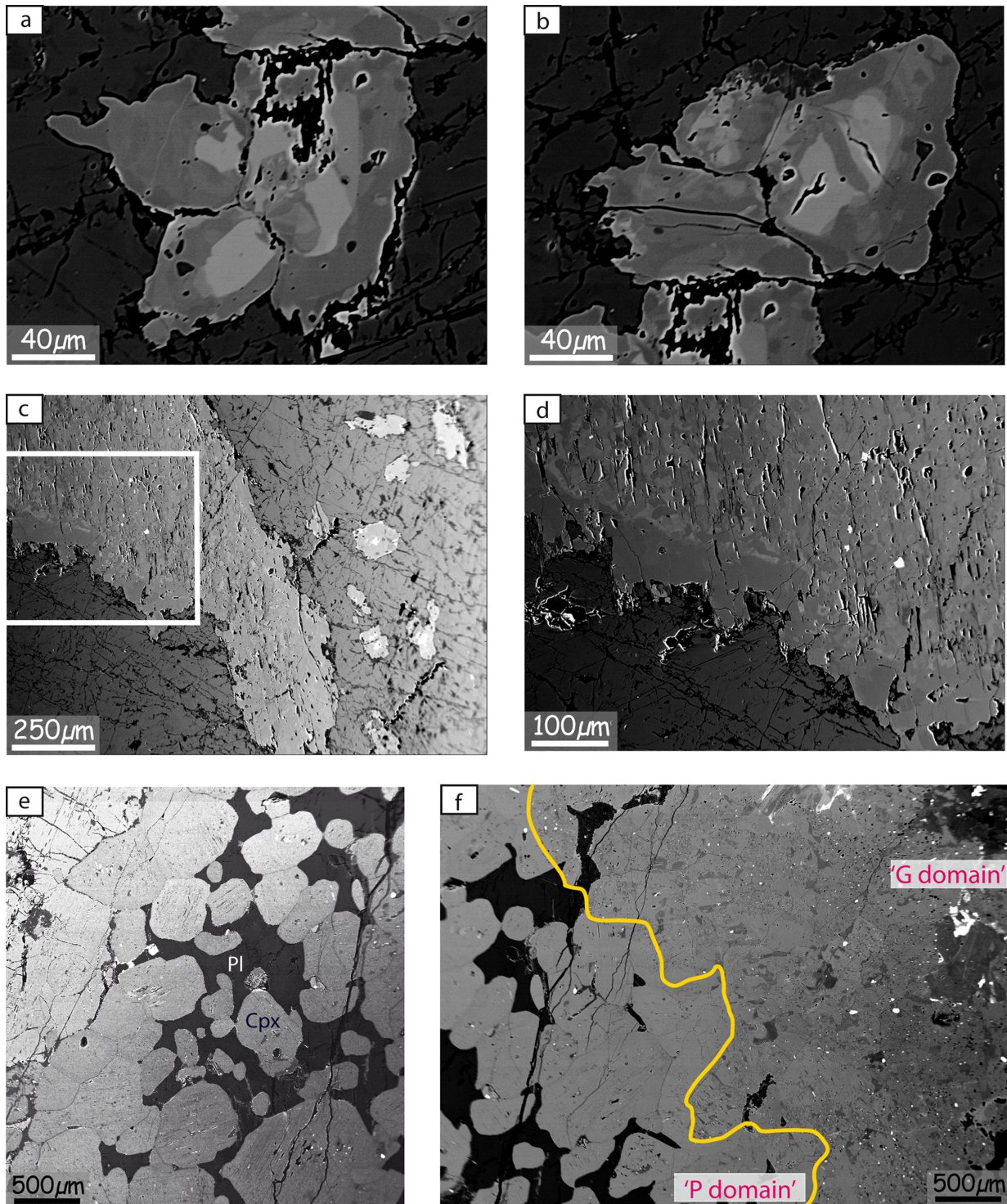


Figure 5. (a–d) Backscattered images of sample 07OL34 and (e and f) backscattered images of sample 07OL36. Figures 5a and 5b: zoned clinopyroxene inclusions in a plagioclase grain. Note that the contact between the core (iron enriched) and the margin (magnesium enriched) is sharp. Figures 5c and 5d: large clinopyroxene grain displaying a heterogeneous core and a homogeneous margin (magnesium enriched), localization of (Figure 5d) picture is highlighted by the square in Figure 5c. Figure 5e: P domain displaying poikilitic plagioclase containing chadacrysts of granular oxide-free clinopyroxene grains; Figure 5f: contact between P domain (to the left) and G domain (to the right); P domain is composed of poikilitic plagioclase containing granular Al-Ti-rich and oxide-free clinopyroxene grains, and G domain is nearly exclusively composed of oxide-bearing low-Al-Ti-clinopyroxenes and subordinated amphiboles.



Table 1. Mineral Compositions (weight %) of Samples 07OL34 and 07OL36 From the Rajmi Area of the Oman Ophiolite^a

Mineral	Comment	SiO ₂	Al ₂ O ₃	TiO ₂	CaO	Na ₂ O	K ₂ O	MnO	MgO	FeO	Cr ₂ O ₃	NiO	Total	<i>n</i>	Mg #	An%	
<i>07OL34</i>																	
AVG Cpx	Large grain rim	54.5	0.69	0.07	25.17	0.15	0.00	0.07	16.99	2.59	0.04	0.01	100.26	32	92	-	
±		0.6	0.30	0.05	0.32	0.04	0.00	0.03	0.32	0.49	0.04	0.01	0.74	-	1	-	
AVG Cpx	Inclusion rim	54.1	1.28	0.18	25.08	0.21	0.00	0.07	16.58	2.70	0.02	0.02	100.24	15	92	-	
±		0.8	0.98	0.20	0.53	0.12	0.00	0.04	0.63	0.61	0.03	0.01	0.63	-	2	-	
AVG Cpx	Large grain core	54.0	0.59	0.10	24.84	0.17	0.00	0.16	16.03	4.88	0.05	0.00	100.76	36	85	-	
±		0.5	0.24	0.06	0.53	0.07	0.00	0.04	0.51	0.81	0.05	0.00	0.72	-	2	-	
AVG Cpx	Inclusion core	52.6	1.25	0.26	23.41	0.30	0.00	0.26	14.42	7.65	0.01	0.00	100.20	9	77	-	
±		0.6	0.19	0.09	0.60	0.03	0.00	0.07	0.57	1.00	0.02	0.00	0.26	-	3	-	
AVG Pl	An _{max} = 99	44.1	35.79	0.00	19.51	0.50	0.00	0.01	0.01	0.06	0.01	0.01	99.98	32	-	96	
±		1.5	0.93	0.01	1.15	0.71	0.00	0.01	0.02	0.03	0.02	0.01	0.43	-	-	6	
AVG Amp	T _{max} = 841°C	50.9	5.42	0.78	12.67	0.87	0.03	0.12	17.77	8.91	0.19	0.00	97.66	37	84	-	
±		2.9	2.33	0.55	0.33	0.48	0.04	0.03	1.39	1.03	0.17	0.00	0.58	-	2	-	
<i>07OL36</i>																	
AVG Cpx	P domains	52.3	1.93	0.39	22.02	0.29	0.00	0.19	14.79	7.86	0.24	0.02	100.00	26	77	-	
±		0.4	0.19	0.10	0.38	0.02	0.00	0.03	0.33	0.35	0.05	0.01	0.34	-	1	-	
AVG Cpx	G domains	53.2	0.86	0.19	23.13	0.20	0.00	0.20	15.01	7.36	0.10	0.01	100.28	34	78	-	
±		0.5	0.31	0.09	0.82	0.06	0.00	0.03	0.36	0.42	0.05	0.01	0.31	-	1	-	
AVG Cpx	Cpx rims at G domains margins	51.9	1.84	0.45	22.15	0.27	0.00	0.17	15.09	7.99	0.16	-	100.01	4	77	-	
±		0.2	0.26	0.06	0.24	0.02	0.00	0.03	0.15	0.16	0.06	-	0.22	-	0	-	
AVG Opx		54.4	1.20	0.13	1.14	0.01	0.00	0.35	24.63	18.50	0.11	0.02	100.49	19	70	-	
±		0.4	0.22	0.06	0.37	0.01	0.00	0.04	0.82	1.19	0.02	0.01	0.31	-	2	-	
AVG Pl	An _{max} = 93	45.9	34.09	0.01	17.95	1.36	0.03	0.01	0.01	0.39	0.01	0.00	99.79	39	-	88	
±		0.8	0.70	0.01	0.61	0.35	0.02	0.01	0.01	0.07	0.02	0.01	0.50	-	-	3	
AVG Amp	T _{max} = 780°C	52.1	4.39	0.76	11.66	0.70	0.09	0.18	17.56	10.12	0.20	0.02	97.79	42	79	-	
±		3.0	2.37	0.55	1.01	0.45	0.07	0.11	1.70	1.87	0.12	0.02	0.40	-	4	-	
AVG Magt		1.3	0.20	0.35	0.78	0.02	0.00	0.19	0.39	83.26	3.80	-	90.30	15	-	-	
±		2.7	0.18	0.25	0.75	0.02	0.01	0.11	0.79	3.36	1.72	-	2.14	-	-	-	
AVG Ilm		0.2	0.02	51.13	0.71	0.01	0.00	2.50	0.20	43.85	0.13	-	98.74	6	-	-	
±		0.1	0.01	0.89	0.19	0.01	0.01	0.97	0.11	1.13	0.07	-	0.87	-	-	-	
AVG Qz		99.7	0.03	0.04	0.02	0.01	0.00	0.01	0.00	0.03	0.03	-	99.88	23	-	-	
±		0.2	0.01	0.01	0.02	0.01	0.00	0.01	0.01	0.06	0.04	-	0.21	-	-	-	

^aAbbreviations: *n*, number of analyses; AVG, average; +/-, standard deviation; Mg #, Mg/(Mg+Fe) x100 in moles; An%, Ca/(Ca+Na+K) x100 in moles; -, not analyzed or below detection limit; Cpx, clinopyroxene; Pl, plagioclase; Ilm, ilmenite; Amp, amphibole; Opx, orthopyroxene; magt, magnetite; Qz, quartz.

temperature estimation using the Al in clinopyroxene thermometer of *France et al.* [2010] reveals an average of 815°C ± 40°C for cores and rims. Temperature estimations using the semiquantitative thermometer of *Ernst and Liu* [1998] based on Ti content in amphibole reveal equilibrium temperatures up to 840°C for hornblendes. In 07OL36, temperature estimations using the semiquantitative thermometer of *Ernst and Liu* [1998] are up to 780°C for hornblendes. Temperature estimations using the two-pyroxene thermometer of *Andersen et al.* [1993] reveal 895°C ± 45°C by applying to the P domains clinopyroxenes and 860°C ± 65°C by applying to the G domains clinopyroxenes that bear oxide inclusions. Temperature estimations using the Al in clinopyroxene thermometer of *France et al.* [2010] reveal 920°C for the P domains clinopyroxenes and 820°C for the G domains oxide-bearing clinopyroxenes.

4. Discussion

4.1. Clues for a Hydrous Crystallizing Magma

[14] Although they represent only minor amounts of the recovered lithologies in present-day oceanic

crust and in ophiolites, samples containing high-An content plagioclases, high-Mg # clinopyroxenes, and/or the presence of clinopyroxene crystallizing before plagioclase are commonly described [e.g., *Sinton et al.*, 1993; *Nielsen et al.*, 1995; *Pan and Batiza*, 2003; *Ridley et al.*, 2006; *Cordier et al.*, 2007; *Koepke et al.*, 2009]. Such peculiar petrologic characteristics carry important information on processes occurring at least locally within the magma chambers of oceanic ridges, especially concerning the hydrous or wet nature of magma.

[15] The occurrence of clinopyroxene inclusions in 07OL34 plagioclases and of poikilitic plagioclases containing granular clinopyroxenes (P domains) in 07OL36 (Figures 4–6) highlights the late crystallization of plagioclase with respect to clinopyroxene. This feature is not characteristic of typical shallow pressures dry MORB melts that crystallize plagioclase first followed by clinopyroxene [e.g., *Grove and Bryan*, 1983]. Alternatively, it is described in magmas from subduction settings where water activities are high [e.g.,

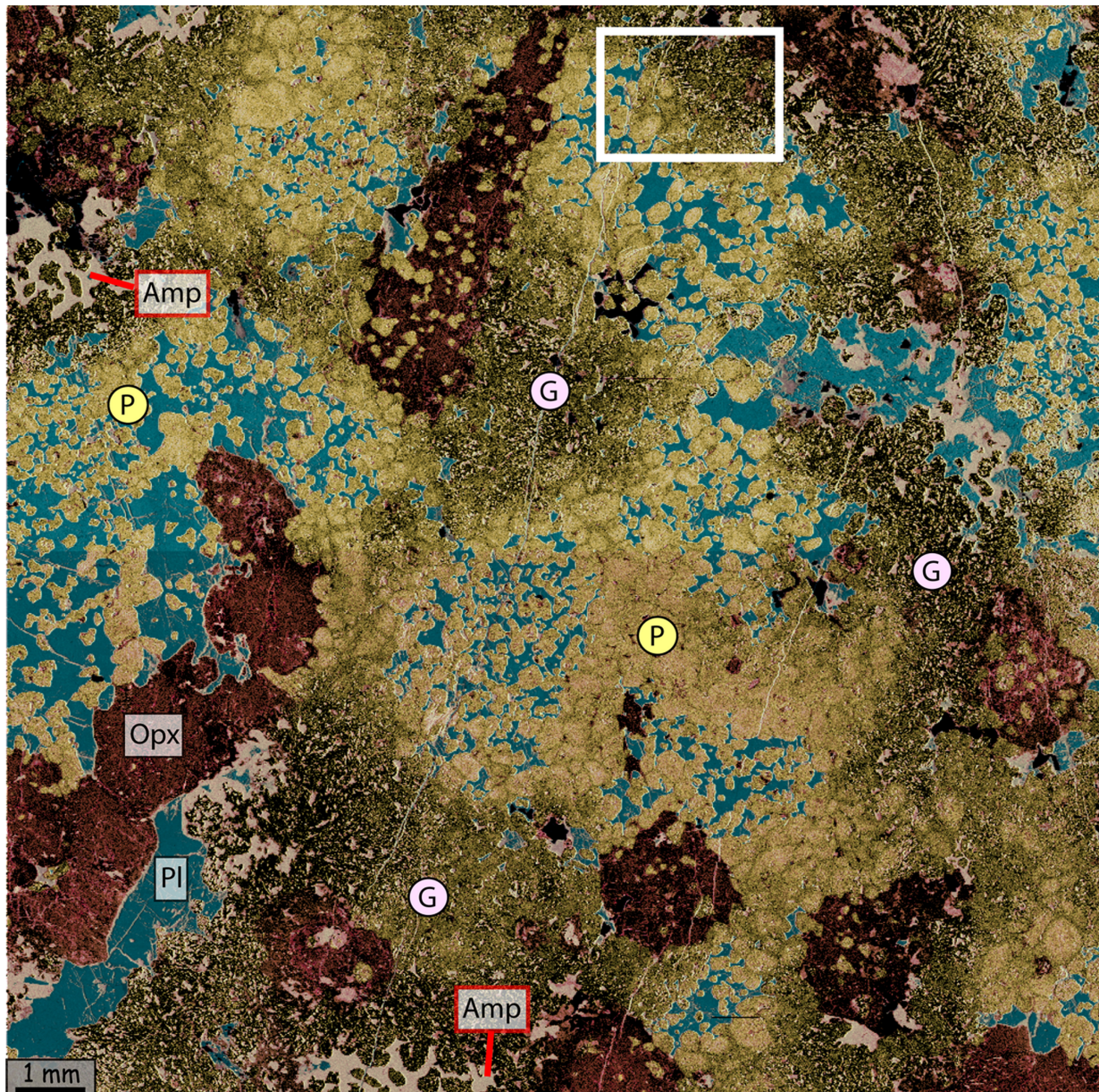


Figure 6. Compositional image (Al+Ca+Mg) of sample 07OL36 (image width: 1.5cm). Blue: plagioclase; yellow: granular oxide-free clinopyroxene (P domains); green: clinopyroxene containing tiny oxide inclusions (G domains); red: orthopyroxene; purple: amphibole. Note the patchy texture with roundish P and G domains. Poikilitic amphibole, plagioclase, and orthopyroxene grains are observed. The white box indicates the location of the picture in Figure 5f.

Gaetani *et al.*, 1993]. The early crystallization of clinopyroxene is also observed in the crystallization of evolved MORB melts (Mg # = 52) in water-rich environments corresponding to highly oxidizing conditions [Berndt *et al.*, 2005], in the crystallization of primitive tholeiitic basalts under high water activities and oxidizing conditions [Feig *et al.*, 2006], and during the hydrous partial melting of previously altered dikes [France *et al.*, 2010]. Thus, the early crystallization of clinopyr-

oxene with respect to plagioclase in ocean ridge related melts at shallow pressures is always associated to high water activities. In 07OL36, the poikilitic texture of some single-grain hornblendes, containing granular clinopyroxenes (Figure 6), points to their magmatic origin and also support the model of crystallization of a hydrous melt. Maximum temperature estimates for these amphiboles are up to 780°C and likely record a subsolidus equilibration; probably indicating a

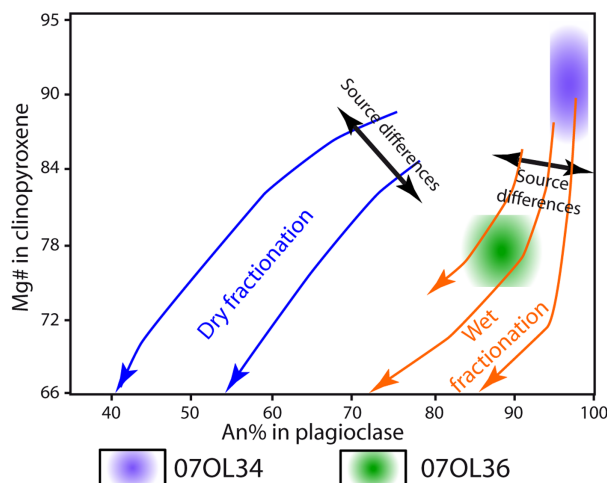


Figure 7. Mg # in clinopyroxene versus An content of plagioclase [after *Kvassnes et al.*, 2004]; the dry and wet fractionation trends are calculated using MELTS [*Ghiorso and Sack*, 1995]; both fractionation trends are calculated for different initial compositions. The studied samples (07OL34 and 07OL36) are typical for the wet fractionation trend. For 07OL34 and 07OL36, plotted are densities of analytical points.

reequilibration during the retrograde evolution. The crystallization of prismatic orthopyroxene (as in 07OL36) in fast-spreading oceanic settings where crystallization occurs at shallow pressures (0.5–2 kb) is usually associated with high silica activity melts and can occur at relatively low temperature if fractional crystallization proceeds (100°C–200°C below the dry solidus temperature of primitive MORB [*Feig et al.*, 2006, 2010]). Therefore, orthopyroxene occurrence in gabbros implies either evolved melts or hydrous conditions able to lower the solidus temperature. Since the investigated gabbros show rather primitive mineral compositions (high Mg # in pyroxene, high An contents in plagioclase), it is obvious that the presence of prismatic orthopyroxene is not a consequence of an evolved bulk composition, implying that they crystallized from a hydrous magma.

[16] Mineral major element compositions, especially those of clinopyroxene and plagioclase, are peculiar and also uncommon for MORB systems. Clinopyroxene Mg # is up to 96 in 07OL34 and up to 82 in 07OL36, while plagioclase An contents are up to 99 in 07OL34 and up to 93 in 07OL36. These values are clearly higher than those of minerals in typical dry MORB systems. They can be attributed either to Mg–Ca rich melts nearly free of Fe–Na [*Panjasawatong et al.*, 1995; *Kohut and Nielsen*, 2003; *Ridley et al.*, 2006] or to the crystallization under high water activities [e.g., *Hattori*

and *Sato*, 1996; *Kuritani*, 1998; *Ginibre et al.*, 2002; *Landi et al.*, 2004; *Feig et al.*, 2006; *Cordier et al.*, 2007; *Koepke et al.*, 2009]. The occurrence of a gabbro xenolith recovered in basalts at the East Pacific Rise [*Ridley et al.*, 2006], which contain high-An plagioclase, has been attributed to the crystallization of a Ca-supra rich melt, principally because water-rich magmas are supposed to be unexpected at oceanic spreading centers [e.g., *Michael and Chase*, 1987]. Nevertheless, such Ca-rich melts (or Ca–Mg-rich melts) have never been sampled or inferred in the upper sections of fast-spreading ridges, a level at which heterogeneous melts produced within the mantle section are well mixed altogether. Alternatively, recent studies [e.g., *Coogan*, 2003; *Cordier et al.*, 2007; *Nicolas et al.*, 2008; *France et al.*, 2009, 2010; *Koepke et al.*, 2011] have highlighted that hydrous melts are present in the uppermost levels of oceanic ridges magmatic systems. *Kvassnes et al.* [2004] performed thermodynamic calculations by using MELTS [*Ghiorso and Sack*, 1995] to model dry and hydrous MORB fractionation trends for different initial compositions (MORB from mid-Atlantic and south-west Indian ridges); results are reported in Figure 7 together with mineral compositions of 07OL34 and 07OL36. The studied samples mineral compositions clearly point to a wet fractionation trend (Figure 7).

[17] The special petrographic features of the investigated gabbros, in particular the uncommon crystallization sequence and the peculiar mineral compositions, emphasize the central role of water during crystallization. Although the hydrated nature of the melt is established, the origin of the sources of hydration remains unclear and has yet been constrained.

4.2. What Is the Hydrous Component Origin? Probably Recycling

[18] Water in magmatic system of mid-ocean ridges may either primarily come from the mantle (“magmatic fluids”) or from hydrothermal fluids derived from seawater [e.g., *Michael and Cornell*, 1998; *Coogan et al.*, 2003; *Nicolas and Mainprice*, 2005; *France et al.*, 2009; *Abily et al.*, 2011]. One possibility of introducing hydrothermal fluids within the magmatic system is recycling/assimilation of previously hydrothermally altered rocks that may suffer hydrous anatexis [*Michael and Schilling*, 1989; *Coogan et al.*, 2003; *France et al.*, 2009, 2010; *Koepke et al.*, 2011]. Recycling may occur in peculiar tectonic settings of oceanic ridges as propagating ridge segment

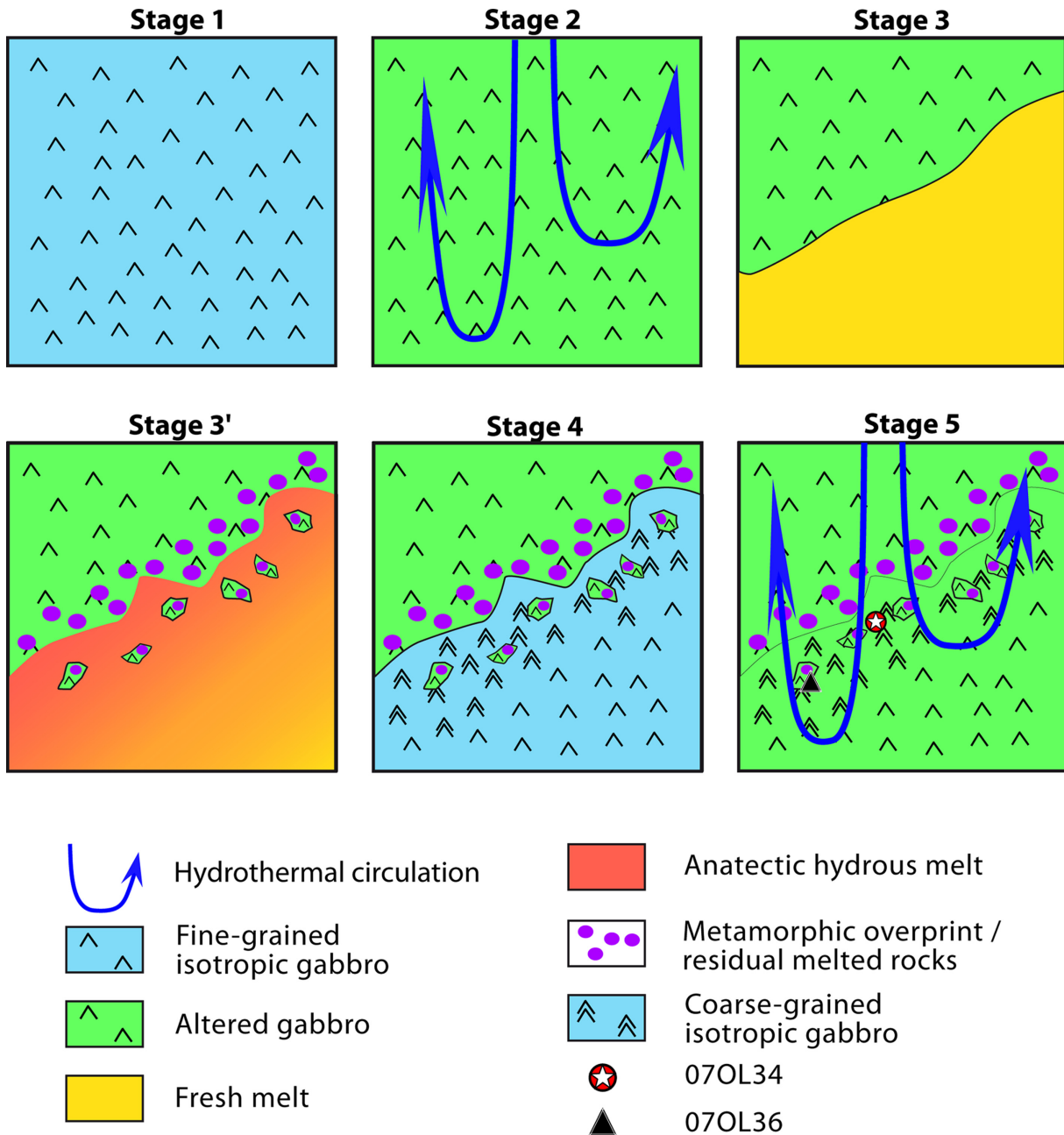


Figure 8. General schematic model for the genesis of the studied hydrous-melt derived coarse-grained gabbros. Stage 1: fine-grained isotropic gabbro crystallization from a MORB-like melt; Stage 2: hydrothermal circulation and partial alteration of the stage 1 gabbro; Stage 3: melt intrusion within the crystallized fine-grained isotropic gabbro, this new melt can either represent an upwelling or growing up of the upper melt lens [e.g., France *et al.*, 2009] or a propagation of a ridge segment close to the end of ridge segment [e.g., Wanless *et al.*, 2010] or to a second magmatic stage related to the early obduction during ophiolite emplacement [e.g., Koepke *et al.*, 2009]. Stage 3': the melt intrusion within the previously hydrothermally altered gabbro triggers the reheating of gabbro and results in its hydrous partial melting; products are a hydrous partial melt and a residual reheated-gabbroic assemblage (observed close to the intrusive contact or as enclaves). The formed hydrous melt can mix with the “fresh melt” of Stage 3 to form a hybridized melt. Stage 4: hybridized hydrous melt crystallizes the coarse-grained gabbros, and dry melt crystallizes the fine-grained gabbros. Some residual assemblages are trapped within the crystallizing gabbros. Stage 5: hydrothermal circulation and partial alteration of all the lithologies. The triangle and the star highlight the possible location of samples 07OL36 and 07OL34, respectively.

tips [Boudier *et al.*, 2000; Wanless *et al.*, 2010], during interactions between melt and hydrothermally altered host rocks at magma chamber roofs

[e.g., Gillis and Coogan, 2002; France *et al.*, 2009; Koepke *et al.*, 2011], or during the shallow subduction occurring in the early obduction in the

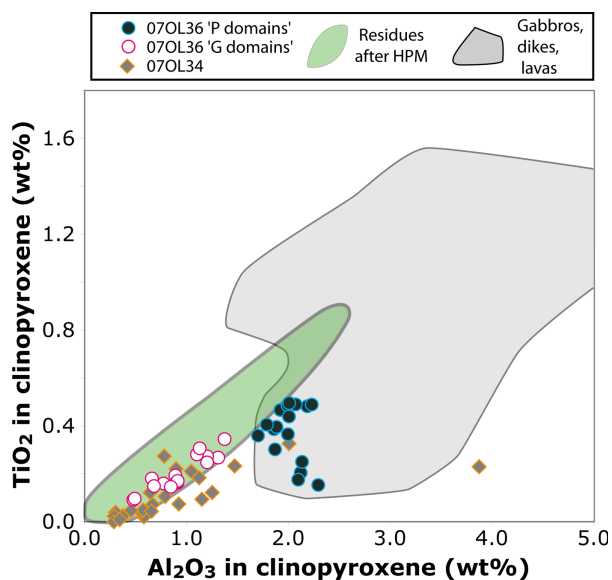


Figure 9. Correlation between TiO_2 and Al_2O_3 in clinopyroxenes. The studied samples (07OL34 and 07OL36; plotted are individual analyses) are compared with clinopyroxenes in residual lithologies formed after the hydrous partial melting of a hydrothermally altered sheeted dike rock (green field noted “Residues after HPM”; compositions from *France et al.* [2009] for natural rocks, and from *France et al.* [2010] for experimental ones) and to experimental and natural data from oceanic crust lithologies (gray field noted “Gabbros, dikes, lavas” from *France et al.* [2009, and references therein]).

case of ophiolites [e.g., *Boudier et al.*, 1985; *Boudier et al.*, 1988; *Koepke et al.*, 2009]. Petrological and geochemical data presented herein can be used to decipher the origin of the hydrous component.

[19] In sample 07OL36, oxide-bearing clinopyroxene domains (G domains) are of interest to identify the hydration source (Figures 4e, 4f, 5f, and 6). The origin of the tiny oxide inclusions within clinopyroxenes can be attributed either to low-temperature alteration occurring during the retrograde evolution [*Manning and MacLeod*, 1996] or to prograde recrystallization after hydrothermal amphibole (i.e., during a reheating stage; *France et al.* [2009, 2010]). The mineralogical distribution in the sample, with two different domains (P and G domains) can be used to discuss further the origin of these oxide inclusions. In the P domains, oxide-free clinopyroxenes are isolated from late-percolating hydrothermal fluids by the poikilitic plagioclases hosting these clinopyroxenes and therefore did not suffer alteration. However, in transitional zones between P and G domains, some oxide-bearing clinopyroxenes are also included in unaltered poikilitic plagioclases; such clinopyrox-

enes have therefore not suffered late hydrothermal alteration, and oxides cannot be attributed to low temperature alteration. Therefore, we suggest that oxide-bearing clinopyroxenes are the products of prograde metamorphism (that may attain anatexis for temperature $>850^\circ\text{C}$ according to *France et al.* [2010]), and replace previous amphibole after a reheating stage [*France et al.*, 2009, 2010]. It also implies an earlier origin of oxide-bearing clinopyroxenes with respect to the poikilitic plagioclases. This chronology is supported by the occurrence at G domain margins, of some oxide-bearing clinopyroxenes displaying rims with similar compositions to the oxide-free clinopyroxenes of P domains (Table 1). A secondary origin of the P domains (oxide-free clinopyroxenes and associated poikilitic plagioclases), with respect to the G domains (oxide-bearing granular clinopyroxenes) is therefore attested.

[20] The absence of plagioclase in G domains is also striking (Figures 5f and 6). The hydrous partial melting of previously hydrothermally altered rocks leads to the stabilization of clinopyroxene at higher temperature than plagioclase and therefore produces clinopyroxenitic residue [*France et al.*, 2010]. During such a hydrous partial melting stage, the recrystallization of clinopyroxene after amphibole leads to the occurrence of oxide-bearing clinopyroxene similar to those observed in G domains [*France et al.*, 2010]. The G domains are therefore interpreted as representing a residue from the hydrous partial melting of a previously hydrothermally altered protolith. This hydrous partial melting stage therefore produces a residual assemblage (G domains), and a hydrous melt. The corresponding anatectic hydrous melt can mix with surrounding MORB melts in the melt lens, producing hybrid hydrous melts that represent a potential contaminating component (Figure 8); this would be characterized by enrichment in elements characteristic for hydrothermal systems such as Cl, Ba, Sr, F, Be, B, etc. [e.g., *Michael and Schilling*, 1989; *Michael and Cornell*, 1998; *Le Roux et al.*, 2006; *Wanless et al.*, 2010]. Such hybrid hydrous melts have the potential to crystallize the surrounding P domains where clinopyroxene crystallizes before plagioclase, and where mineral compositions attest to a water-rich environment (Figure 8).

[21] Clinopyroxene from the two domains have different compositions, which is consistent with the proposed scenario (Figures 8 and 9). Residual clinopyroxenes from G domains have lower Cr_2O_3 and Al_2O_3 contents than the magmatic clinopyroxenes from P domains. These lower Cr_2O_3 and

Al₂O₃ contents are consistent with a lower temperature equilibration [Koepke *et al.*, 2008; France *et al.*, 2010]. Another clue for a recycled origin of the G domains clinopyroxenes is their compositional similarity with residual clinopyroxenes formed by melting hydrothermally altered dikes either in natural settings or experimentally (Figure 9) [France *et al.*, 2009, 2010]. Conversely, P domain clinopyroxenes display compositions that do not correspond to the ones of residual clinopyroxenes and are therefore interpreted as magmatic (Figure 9). Temperature estimations performed using the two-pyroxene thermometer [Andersen *et al.*, 1993] and using the Al in clinopyroxene thermometer [France *et al.*, 2010] also give higher temperature for the P domain clinopyroxenes, than for the G ones, consistent with a magmatic origin of P. The coarse grain size in G domains is consistent with a gabbroic protolith, rather than with a dike protolith (Figure 8), and the presence of leucocratic veins in the surrounding gabbros (Figure 3) may also support that those surrounding lithologies have suffered anatexis [e.g., Koepke *et al.*, 2004].

[22] In sample 07OL34, the crystallization sequence and the mineral compositions imply high water activities; such water activities could result from a strong fractionation event that would concentrate magmatic fluids in the residual melt, which must then show a much evolved composition. However, the extreme mineral compositions (high Mg # in clinopyroxene and An% up to 99) imply a relatively primitive nature of the hydrous melt. This implies that the hydrous component does not derive from magmatic fluids, but has been added as hydrothermal flux (through magma fluid interactions or through assimilation of previously altered material) to a relatively primitive MORB melt. Sharp and reverse zonations in clinopyroxene inclusions are consistent with either a sudden hydration of magma or an inherited origin of the cores embedded in a hydrous crystallizing melt.

[23] Both large prismatic clinopyroxene grains and the inclusions within the plagioclases display rims enriched in MgO. The zoned clinopyroxene inclusions are hosted in compositionally homogeneous plagioclase grains, implying that those plagioclases grew from a melt in equilibrium with the clinopyroxene rims. Mineral compositions require a hydrous component present during the crystallization of plagioclases and clinopyroxene rims; a hydrous component is not required to obtain the clinopyroxene core compositions.

[24] For gabbro 07OL34, the petrographic and mineral chemical features imply the following

two-stage scenario. Either a relatively primitive dry melt has crystallized clinopyroxene cores, followed by a second stage where the melt was suddenly hydrated, or the clinopyroxene cores result from the partial assimilation and anatexis of previously altered rocks within an intruding magma. The two proposed scenarios involve a second stage with a relatively primitive hydrous melt that cannot be produced by classical MORB extreme fractionation and which require an input of hydrothermal fluids. Such hydrothermal fluxes may be incorporated to ridge axis primitive melts by different processes: (1) during magma-hydrothermal interactions where fresh magmas assimilate hydrous anatectic melts as described in Oman, Troodos, and at the East Pacific Rise close to magma chamber roofs [e.g., Coogan *et al.*, 2003; Gillis *et al.*, 2003; France *et al.*, 2009, 2010; Wanless *et al.*, 2010]; (2) by injecting fresh magmas in previously hydrothermally altered crust that may suffer anatexis close to propagating oceanic ridge segment terminations [e.g., Boudier *et al.*, 2000; Wanless *et al.*, 2010]; (3) or during the initiation of obduction process [e.g., Ishikawa *et al.*, 2002; Yamasaki *et al.*, 2006; Koepke *et al.*, 2009].

4.3. General Implications and Conclusions

[25] The present study sheds light on a process that generates coarse-grained gabbro in oceanic settings, in the transition zone between the lower igneous crust and the upper extrusive crust. We show that high water activities are required to generate the peculiar petrology and mineral compositions of the studied samples. This water-rich fluid probably derives from the recycling and anatexis of previously hydrothermally altered rocks (Figure 8). The coarse-grained characteristic may also result from this high water activity peculiarity as high water activities result in very large, fast-growing crystals (by decreasing the nucleation rate and thus producing substantial undercooled conditions [Nabelek *et al.*, 2010]).

[26] Three processes are proposed here to trigger the recycling episode: (1) interactions between the hydrothermal and magmatic convecting systems at the magma chamber roof, resulting in the genesis of an anatectic hydrous melt that may mix with MORB magmas [France *et al.*, 2009, 2010; Koepke *et al.*, 2011]; (2) propagating ridge segment tips into previously cooled and hydrothermally altered crust, also resulting in the genesis of an anatectic hydrous melt [Boudier *et al.*, 2000; Wanless *et al.*, 2010]; (3) intrusion of hydrous



melts produced by fluid-enhanced melting of previously depleted mantle during the early obduction [Ishikawa *et al.*, 2002; Yamasaki *et al.*, 2006; Koepke *et al.*, 2009]. All of these processes have the potential to recycle hydrothermally altered rocks (e.g., sheeted dikes, gabbros) and could locally produce wet magmatism at oceanic spreading centers. Both (1) and (2) take place in present day oceanic crust and represent widespread processes that have been observed in different sites (e.g., East Pacific Rise, Juan de Fuca Ridge). While igneous processes at oceanic spreading centers are mostly dry, wet magmatism does also occur [Michael and Schilling, 1989; Michael and Cornell, 1998; Nielsen *et al.*, 2000; Koepke *et al.*, 2004, 2005a, 2005b, 2007, 2011; Berndt *et al.*, 2005; Cordier *et al.*, 2007; France *et al.*, 2009, 2010; Abily *et al.*, 2011; this study], can be generated by various processes and may contribute to the geochemical signals that are borne by MORBs.

Acknowledgments

[27] The authors thank Christophe Nevado and Dorianne Delmas (Géosciences Montpellier) for the quality of the thin sections. They also thank Claude Merlet (Géosciences Montpellier) for assistance during electron probe microanalyses. Constructive reviews by two anonymous reviewers are gratefully acknowledged. This research was supported by CNRS-INSU programs 3F and SYSTER (AMISHADOq), the Université Franco-Allemande/Deutsch-Französische Hochschule, and the Région Lorraine. The authors thank the director general of Minerals from the Ministry of Commerce and Industry of the Sultanate of Oman, for allowing us to sample the Oman ophiolite. This is CRPG contribution number 2247.

References

- Abily, B., G. Ceuleneer, and P. Launeau (2011), Synmagmatic normal faulting in the lower oceanic crust: Evidence from the Oman ophiolite, *Geology*, *39*(4), 391–394, doi:10.1130/G31652.1.
- Alabaster, T., J. A. Pearce, and J. Malpas (1982), The volcanic stratigraphy and petrogenesis of the Oman ophiolite complex, *Contrib. Mineral. Petrol.*, *81*, 168–183.
- Andersen, D. J., D. H. Lindsley, and P. M. Davidson (1993), QUILF: A Pascal program to assess equilibria among Fe-Mg-Mn-Ti oxides, pyroxenes, olivine, and quartz, *Comput. Geosci.*, *19*, 1333–1350, doi:10.1016/0098-3004(93)90033-2.
- Benoit, M., G. Ceuleneer, and M. Polvé (1999), The remelting of hydrothermally altered peridotite at mid-ocean ridges by intruding mantle diapirs, *Nature*, *402*, 514–518, doi:10.1038/990073.
- Berndt, J., J. Koepke, and F. Holtz (2005), An experimental investigation of the influence of water and oxygen fugacity on differentiation of MORB at 200 MPa, *J. Petrol.*, *46*, 135–167.
- Bosch, D., M. Jamais, F. Boudier, A. Nicolas, J. M. Dautria, and P. Agrinier (2004), Deep and high temperature hydrothermal circulation in the Oman ophiolite: Petrological and isotopic evidence, *J. Petrol.*, *45–46*, 1181–1208, doi:10.1093/ptrology/egh010.
- Boudier, F., and A. Nicolas (2007), Comment on “Dating the geologic history of Oman’s Semail ophiolite: Insights from U-Pb geochronology” by C. J. Warren, R. R. Parrish, D. J. Waters, and M. P. Searle, *Contrib. Mineral. Petrol.*, *154*, 111–113.
- Boudier, F., J. L. Bouchez, A. Nicolas, M. Cannat, G. Ceuleneer, M. Misseri, and R. Montigny (1985), Kinematics of oceanic thrusting in the Oman ophiolite—Model of plate convergence, *Earth Planet. Sci. Lett.*, *75*, 215–222, doi:10.1016/0012-821X(85)90103-7.
- Boudier, F., G. Ceuleneer, and A. Nicolas (1988), Shear zones, thrusts and related magmatism in the Oman ophiolite: Initiation of thrusting at an ocean ridge, *Tectonophysics*, *151*, 275–296.
- Boudier, F., A. Nicolas, and B. Ildefonse (1996), Magma chambers in the Oman ophiolite: Fed from the top and the bottom, *Earth Planet. Sci. Lett.*, *144*, 239–250, doi:10.1016/0012-821X(96)00167-7.
- Boudier, F., M. Godard, and C. Armbruster (2000), Significance of gabbro-norite occurrence in the crustal section of the Semail ophiolite, *Mar. Geophys. Res.*, *21*, 307–326, doi:10.1023/A:1026726232402.
- Coogan, L. A. (2003), Contaminating the lower crust in the Oman ophiolite, *Geology*, *31*(12), 1065–1068, doi:10.1130/G20129.1.
- Coogan, L. A., N. C. Mitchell, and M. J. O’Hara (2003), Roof assimilation at fast spreading ridges: An investigation combining geophysical, geochemical, and field evidence, *J. Geophys. Res.*, *108*(B1), 2002, doi:10.1029/2001JB001171.
- Cordier, C., M. Caroff, T. Juteau, C. Fleutelot, C. Hémond, M. Drouin, J. Cotton, and C. Bollinger (2007), Bulk-rock geochemistry and plagioclase zoning in lavas exposed along the northern flank of the Western Blanco Depression (Northeast Pacific): Insight into open-system magma chamber processes, *Lithos*, *99*, 289–311.
- Detrick, R.S., P. Buhl, E. Vera, J. Mutter, J. Orcutt, J. Madsen, and T. Brocher (1987), Multichannel seismic imaging of a crustal magma chamber along the East Pacific Rise, *Nature*, *326*, 35–41.
- Ernewein, M., C. Pflumio, and H. Whitechurch (1988), The death of an accretion zone as evidenced by the magmatic history of the Semail ophiolite (Oman), *Tectonophysics*, *151*, 247–274.
- Ernst, W.G., and J. Liu (1998), Experimental phase-equilibrium study of Al- and Ti-contents of calcic amphibole in MORB—A semiquantitative thermobarometer, *Am. Mineral.*, *83*, 952–969.
- Feig, S. T., J. Koepke, and J. E. Snow (2006), Effect of water on tholeiitic basalt phase equilibria: An experimental study under oxidizing conditions, *Contrib. Mineral. Petrol.*, *152*(5), 611–638, doi:10.1007/s00410-006-0123-2.
- Feig, S. T., J. Koepke, and J. E. Snow (2010), Effect of oxygen fugacity and water on phase equilibria of a hydrous tholeiitic basalt, *Contrib. Mineral. Petrol.*, *159*, 551–568, doi:10.1007/s00410-010-0493-3.
- France, L. (2009), *Magmatic/hydrothermal interactions at fast spreading mid-ocean ridges: Implications on the dynamics of the axial melt lens*, PhD dissertation, Géosci. Montpellier, Univ. de Montpellier II, Montpellier, France. [Available at <http://tel.archives-ouvertes.fr/tel-00448699>.]

- France, L., B. Ildefonse, and J. Koepke (2009) Interactions between magma and hydrothermal system in Oman ophiolite and in IODP Hole 1256D: Fossilization of a dynamic melt lens at fast spreading ridges, *Geochem. Geophys. Geosyst.*, *10*, Q10O19, doi:10.1029/2009GC002652.
- France, L., J. Koepke, B. Ildefonse, S. B. Cichy, and F. Deschamps (2010), Hydrous partial melting in the sheeted dike complex at fast spreading ridges: experimental and natural observations, *Contrib. Mineral. Petrol.*, *160–165*, 683–704.
- Gaetani, G. A., T. L. Grove, and W. B. Bryan (1993), The influence of water on the petrogenesis of subduction-related igneous rocks, *Nature*, *365*, 332–334.
- Ghiorso, M. S., and R. O. Sack (1995), Chemical mass transfer in magmatic processes. IV. A revised and internally consistent thermodynamic model for the interpolation of liquid–solid equilibria in magmatic systems at elevated temperatures and pressures, *Contrib. Mineral. Petrol.*, *119*, 197–212.
- Gillis, K.M. (2008), The roof of an axial magma chamber: A hornfelsic heat exchanger, *Geology*, *36*, 299–302, doi:10.1130/G24590A.1.
- Gillis, K. M., and L. A. Coogan (2002), Anatexitic migmatites from the roof of an ocean ridge magma chamber, *J. Petrol.*, *43*, 2075–2095, doi:10.1093/petrology/43.11.2075.
- Gillis, K. M., L. A. Coogan, and M. Chaussidon (2003), Volatile element (B, Cl, F) behavior in the roof of an axial magma chamber from the East Pacific Rise, *Earth Planet. Sci. Lett.*, *213*, 447–462.
- Ginibre, C., G. Wörner, and A. Kronz (2002), Minor- and trace-element zoning in plagioclase: Implications for magma chamber processes at Paríacota volcano, northern Chile, *Contrib. Mineral. Petrol.*, *143*, 300–315.
- Godard, M., J. M. Dautria, and M. Perrin (2003), Geochemical variability of the Oman ophiolite lavas: Relationship with spatial distribution and paleomagnetic directions, *Geochem. Geophys. Geosyst.*, *4*(6), 8609, doi:10.1029/2002GC000452.
- Grove, T. L., and W. B. Bryan (1983), Fractionation of pyroxene-phyric MORB at low pressure: An experimental study, *Contrib. Mineral. Petrol.*, *84*, 293–309.
- Hattori, K., and H. Sato (1996), Magma evolution recorded in plagioclase zoning in 1991 Pinatubo eruption products, *Am. Mineral.*, *81*, 982–994.
- Hooft, E. E. E., R. S. Detrick, and G. M. Kent (1997), Seismic structure and indicators of magma budget along the Southern East Pacific Rise, *J. Geophys. Res.*, *102*, 27,319–27,340.
- Ishikawa, T., K. Nagaishi, and S. Umino (2002), Boninitic volcanism in the Oman ophiolite: Implications for thermal condition during transition from spreading ridge to arc, *Geology*, *30*, 899–902.
- Kelemen, P. B., K. Koga, and N. Shimizu (1997), Geochemistry of gabbro sills in the crust-mantle transition zone of the Oman ophiolite: Implications for the origin of the oceanic lower crust, *Earth Planet. Sci. Lett.*, *146*, 475–488.
- Kelley, K. A., and E. Cottrell (2009), Water and the oxidation state of subduction zone magmas, *Science*, *325*, 605–607, doi:10.1126/science.1174156.
- Koepke, J., S. T. Feig, J. Snow, and M. Freise (2004), Petrogenesis of oceanic plagiogranites by partial melting of gabbros: An experimental study, *Contrib. Mineral. Petrol.*, *146*, 414–432.
- Koepke, J., S. T. Feig, and J. Snow (2005a), Late stage magmatic evolution of oceanic gabbros as a result of hydrous partial melting: Evidence from the Ocean Drilling Program (ODP) Leg 153 drilling at the Mid-Atlantic Ridge, *Geochem. Geophys. Geosyst.*, *6*, Q02001, doi:10.1029/2004GC000805.
- Koepke, J., S. T. Feig, and J. Snow (2005b), Hydrous partial melting within the lower oceanic crust, *Terra Nova*, *17*, 286–291, doi:10.1111/j.1365–3121.2005.00613.x.
- Koepke, J., J. Berndt, S. T. Feig, and F. Holtz (2007), The formation of SiO₂-rich melts within the deep oceanic crust by hydrous partial melting of gabbros, *Contrib. Mineral. Petrol.*, *153*, 67–84, doi:10.1007/s00410-006-0135-y.
- Koepke, J., D. M. Christie, W. Dziony, F. Holtz, D. Lattard, J. MacLennan, S. Park, B. Scheibner, T. Yamasaki, and S. Yamazaki (2008), Petrography of the Dike/Gabbro transition at IODP site 1256 (Equatorial Pacific): The evolution of the Granoblastic Dikes, *Geochem. Geophys. Geosyst.*, *9*, Q07O09, doi:10.1029/2008GC001939.
- Koepke, J., S. Schoenborn, M. Oelze, H. Wittmann, S. T. Feig, E. Hellebrand, F. Boudier, and R. Schoenberg (2009), Petrogenesis of crustal wehrlites in the Oman ophiolite: Experiments and natural rocks, *Geochem. Geophys. Geosyst.*, *10*, Q10002, doi:10.1029/2009GC002488.
- Koepke, J., L. France, T. Müller, F. Faure, N. Goetze, W. Dziony, and B. Ildefonse (2011), Gabbros from IODP Site 1256, equatorial Pacific: Insight into axial magma chamber processes at fast spreading ocean ridges, *Geochem. Geophys. Geosyst.*, *12*, Q09014, doi:10.1029/2011GC003655.
- Koga, K. T., P. B. Kelemen, and N. Shimizu (2001), Petrogenesis of the crust-mantle transition zone and the origin of lower crustal wehrlite in the Oman ophiolite, *Geochem. Geophys. Geosyst.*, *2*(9), 1038, doi:10.1029/2000GC000132.
- Kohut, E. J., and R. L. Nielsen (2003), Low-pressure phase equilibria of anhydrous anorthite-bearing mafic magmas, *Geochem. Geophys. Geosyst.*, *4*(7), 1057, doi:10.1029/2002GC000451.
- Kuritani, T. (1998), Boundary layer crystallization in a basaltic magma chamber: Evidence from Rishiri volcano, northern Japan, *J. Petrol.*, *39*, 1619–1640.
- Kvassnes, A. J. S., A. H. Strand, H. Moen-Eikeland, and R. B. Pedersen (2004), The Lyngen Gabbro: The lower crust of an Ordovician Incipient Arc, *Contrib. Mineral. Petrol.*, *148*, 358–379.
- Lamoureaux, G., B. Ildefonse, and D. Mainprice (1999), Modelling the seismic properties of fast-spreading ridge crustal low-velocity zones: Insights from Oman gabbro textures, *Tectonophysics*, *312*, 283–301.
- Landi, P., N. Métrich, A. Bertagnini, and M. Rosi (2004), Dynamics of magma mixing and degassing recorded in plagioclase at Stromboli (Aeolian Archipelago, Italy), *Contrib. Mineral. Petrol.*, *147*, 213–227.
- Le Roux, P. J., S. B. Shirey, E. H. Hauri, M. R. Perfit, and J. F. Bender (2006), The effects of variable sources, processes and contaminants on the composition of northern EPR MORB (8–10°N and 12–14°N): Evidence from volatiles (H₂O, CO₂, S) and halogens (F, Cl), *Earth Planet. Sci. Lett.*, *251*, 209–231.
- MacLeod, C. J., and D. A. Rothery (1992), Ridge axial segmentation in the Oman ophiolite: Evidence from along-strike variations in the sheeted dyke complex, in *Ophiolites and Their Modern Analogues*, vol. 60, edited by L. M. Parson, B. J. Murton, and P. Browning, pp. 39–63, Geol. Soc. Spec. Publ., London.
- MacLeod, C. J., and G. Yaouancq (2000), A fossil melt lens in the Oman ophiolite: Implications for magma chamber



- processes at fast spreading ridges, *Earth Planet. Sci. Lett.*, *176*, 357–373, doi:10.1016/S0012-821X(00)00020-0.
- Manning, C. E., and C. J. MacLeod (1996), Fracture-controlled metamorphism of Hess Deep gabbros, Site 894: Constraints on the roots of mid-ocean-ridge hydrothermal systems at fast-spreading centers, in *Proceedings of the Ocean Drilling Program, Scientific Results*, vol. 147, edited by C. Mével, K. M. Gillis, J. F. Allan and P. S. Meyer, pp. 189–212.
- Merlet, C. (1994), An accurate computer correction program for quantitative electron probe microanalysis, *Mikrochim. Acta*, *114–115*, 363–376, doi:10.1007/BF01244563.
- Michael, P. J., and R. L. Chase (1987), The influence of primary magma composition, H₂O and pressure on Mid-Ocean Ridge Basalt differentiation, *Contrib. Mineral. Petrol.*, *96*, 245–263.
- Michael, P. J., and W. C. Cornell (1998), Influence of spreading rate and magma supply on crystallization and assimilation beneath mid-ocean ridges: Evidence from chlorine and major element chemistry of mid ocean ridge basalts, *J. Geophys. Res.*, *103*, 18,325–18,356.
- Michael, P. J., and J. G. Schilling (1989), Chlorine in mid-ocean ridge magmas: Evidence for assimilation of sea water influenced components, *Geochim. Cosmochim. Acta*, *53*, 3131–3143.
- Morton, J. L., and N. Sleep (1985), Seismic reflexions from a Lau Basin magma chamber, in *Geology and Offshore Resources of Pacific Island Arcs—Tonga Region*, *Earth Sci. Ser.*, vol. 2, edited by D. W. Scholl and T. L. Vallier, Circum-Pacific Council for Energy and Mineral Resources, pp. 441–453, Houston, Tex.
- Nabelek, P. I., A. G. Whittington, and M. L. C. Sirbescu (2010), The role of H₂O in rapid emplacement and crystallization of granite pegmatites: Resolving the paradox of large crystals in highly undercooled melts, *Contrib. Mineral. Petrol.*, *160*, 313–325, doi:10.1007/s00410-009-0479-1.
- Natland, J. H., and H. J. B. Dick (1996), *Melt migration through high-level gabbroic cumulates of the East Pacific Rise at Hess Deep: The origin of magma lenses and the deep crustal structure of fast-spreading ridges*, in *Proceedings of the Ocean Drilling Program, Scientific Results*, vol. 147, edited by C. Mével, K. M. Gillis, J. F. Allan, and P. S. Meyer, pp. 21–58, doi: 10.2973/odp.proc.sr.147.002.1996.
- Nicolas, A., and F. Boudier (2008), Large shear zones with no relative displacement, *Terra Nova*, *20*, 200–205, doi:10.1111/j.1365-3121.2008.00806.x.
- Nicolas, A., and D. Mainprice (2005), Burst of high-temperature seawater injection throughout accreting oceanic crust a case study in Oman ophiolite, *Terra Nova*, *17*, 326–330, doi:10.1111/j.1365-3121.2005.00617.x.
- Nicolas, A., F. Boudier, B. Ildefonse, and E. Ball (2000), Accretion of Oman and United Arab Emirates ophiolite: Discussion of a new structural map, *Mar. Geophys. Res.*, *21*, 147–179, doi:10.1023/A:1026769727917.
- Nicolas, A., F. Boudier, J. Koepke, L. France, B. Ildefonse, and C. Mevel (2008), Root zone of the sheeted dike complex in the Oman ophiolite, *Geochem. Geophys. Geosyst.*, *9*, Q05001, doi:10.1029/2007GC001918.
- Nicolas, A., F. Boudier, and L. France (2009), Subsidence in magma chamber and the development of magmatic foliation in Oman ophiolite gabbros, *Earth Planet Sci. Lett.*, *284*, 76–87, doi:10.1016/j.epsl.2009.04.012.
- Nielsen, R. L., J. Crum, R. Bourgeois, K. Hascall, L. M. Forsythe, M. R. Fisk, and D. M. Christie (1995), Melt inclusions in high—An plagioclase from the Gorda Ridge: An example of the local diversity of MORB parent magmas, *Contrib. Mineral. Petrol.*, *122*, 34–50, doi:10.1007/s004100050111.
- Nielsen, R. L., R. E. Sours-Page, and K. S. Harpp (2000), Role of a Cl⁻ bearing flux in the origin of depleted ocean floor magmas, *Geochem. Geophys. Geosyst.*, *1*(5), 1007, doi: 10.1029/1999GC000017.
- Pallister, J. S., and C. A. Hopson (1981), Samail Ophiolite plutonic suite: Field relations, phase variation, cryptic variation and layering, and a model of a spreading ridge magma chamber, *J. Geophys. Res.*, *86*, 2593–2644, doi:10.1029/JB086iB04p02593.
- Pan, Y., and R. Batiza (2003), Magmatic processes under mid ocean ridges: A detailed mineralogic study of lavas from East Pacific Rise 9°30'N, 10°30'N, and 11°20'N, *Geochem. Geophys. Geosyst.*, *4*(11), 8623, doi:10.1029/2002GC000309.
- Panjasawatong, Y., L. V. Danyushevsky, A. J. Crawford, and K. L. Harris (1995), An experimental study of the effects of melt composition on plagioclase-melt equilibria at 5 and 10 kbar: Implications for the origin of high An plagioclase in arc and MORB magmas, *Contrib. Mineral. Petrol.*, *118*, 420–435.
- Phipps Morgan, J., and Y. J. Chen (1993), The genesis of oceanic crust: Magma injection, hydrothermal circulation, and crustal flow, *J. Geophys. Res.*, *98*, 6283–6297.
- Pouchou, J. L., and F. Pichoir (1991), Quantitative analysis of homogeneous or stratified microvolumes applying the model “PAP”, in *Electron Probe Quantification*, edited by K. F. J. Heinrich and D. E. Newbury, pp. 31–75, Plenum, New York.
- Quick, J. E., and R. P. Denlinger (1993), Ductile deformation and the origin of layered gabbro in ophiolites, *J. Geophys. Res.*, *98*, 14,015–14,027.
- Reuber, I. (1988), Complexity of the crustal sequence in the northern Oman ophiolite (Fizh and southern Aswad blocks): The effect of early slicing? *Tectonophysics*, *151*, 137–165.
- Ridley, W. I., M. R. Perfit, M. C. Smith, and D. J. Fornari (2006), Magmatic processes in developing oceanic crust revealed in a cumulate xenolith collected at the East Pacific Rise, 9°50'N, *Geochem. Geophys. Geosyst.*, *7*, Q12004, doi:10.1029/2006GC001316.
- Sinton, J. M., and R. S. Detrick (1992), Mid-ocean ridge magma chambers, *J. Geophys. Res.*, *97*, 197–216, doi: 10.1029/91JB02508.
- Sinton, C. W., D. M. Christie, V. L. Coombs, R. L. Nielsen, and M. R. Fisk (1993), Near-primary melt inclusions in anorthite phenocrysts from the Galapagos Platform, *Earth Planet. Sci. Lett.*, *119*, 527–537, doi:10.1016/0012-821X(93)90060-M.
- Sobolev, A. V., and M. Chaussidon (1996), H₂O concentrations in primary melts from supra-subduction zones and mid-ocean ridges: Implications for H₂O storage and recycling in the mantle, *Earth Planet. Sci. Lett.*, *137*, 45–55.
- Stern, R. J. (2004), Subduction initiation: Spontaneous and induced, *Earth Planet. Sci. Lett.*, *226*, 275–292.
- Usui, Y., and S. Yamazaki (2010), Salvaging primary remanence from hydrothermally altered oceanic gabbros in the Oman ophiolite: A selective destructive demagnetization approach, *Phys. Earth Planet. Inter.*, *181*, 1–11.
- Wanless, V. D., and A. M. Shaw (2012), Lower crustal crystallization and melt evolution at mid-ocean ridges, *Nat. Geosci.*, *5*, 651–655, doi:10.1038/NGEO1552.
- Wanless, V. D., M. R. Perfit, W. I. Ridley, and E. E. Klein (2010), Dacite petrogenesis on mid-ocean ridges: Evidence for oceanic crustal melting and assimilation, *J. Petrol.*, *51*, 2377–2410, doi:10.1093/petrology/egq056.



- Warren, C. J., R. R. Parrish, D. J. Waters, and M. P. Searle (2005), Dating the geologic history of Oman's Semail Ophiolite: Insights from U–Pb geochronology, *Contrib. Mineral. Petrol.*, *150*, 403–422.
- Warren, C. J., M. P. Searle, R. R. Parrish, and D. J. Waters (2007), Reply to comment by F. Boudier and A. Nicolas on “Dating the geologic history of Oman's Semail Ophiolite: Insights from U–Pb geochronology,” *Contrib. Mineral. Petrol.*, *154*, 115–118.
- Wilson, D. S., et al. (2006), Drilling to gabbro in intact ocean crust, *Science*, *312*, 1016–1020, doi:10.1126/science.1126090.
- Wood, B. J., L. T. Bryndzia, and K. E. Johnson (1990), Mantle oxidation state and its relationship to tectonic environment and fluid speciation, *Science*, *248*, 337–345.
- Yamazaki, S., and S. Miyashita (2008), Geochemistry of high-Ca boninite dike swarms and the related plutonic rocks in the Oman ophiolite, Abstract T21A-1939 presented at 2008 Fall Meeting, AGU, Washington, D. C.
- Yamasaki, T., J. Maeda, and T. Mizuta (2006), Geochemical evidence in clinopyroxenes from gabbroic sequence for two distinct magmatisms in the Oman ophiolite, *Earth Planet. Sci. Lett.*, *251*, 52–65, doi:10.1016/j.epsl.2006.08.027.